

FIGURE 19.—Types of fillets. *A*, Concave with steep contact between rock and soil; example is Big rock at station B2 (part of NASA photograph AS14-68-9414). *B*, Low angle with low-dipping contact between rock and soil; example is Saddle rock at station C1

(NASA photograph AS14-68-9450). *C*, Convex under rock overhang; example is Contact rock at station C1 (NASA photograph AS14-68-9448).

been in place. Uncertainties arise because some cratering events are large enough to embank relatively large amounts of material against nearby rocks.

#### OPTICAL PROPERTIES

The polarizing characteristics of lunar materials were measured from earth-based telescopes prior to any of the lunar missions. These measurements are integrated over areas about 300 km<sup>2</sup> and show the degree of polarization varies with phase angle, and that maximum polarization occurs at a phase angle of about 100°. The maximum polarization of incident light varies between about 5 and 20 percent. Although there is a continuum of values, with some overlap between mare and highland materials, the mare materials tend to have higher values of polarization (Dollfus, 1962; Wright and others, 1963; Wilhelms and Trask, 1965; Trask, 1966).

The television cameras flown on the Surveyor 6 and 7 missions had polarizing filters for measuring polarizing characteristics over areas of a few square centimetres to a square metre. Surveyor 6, which landed in Sinus Medii, indicated that the degree of polarization at a phase angle of 100° is about 16–19 percent. Surveyor 7, which landed on the ejecta blanket of the crater Tycho in the southern highlands, showed that the degree of polarization is about 7–9 percent at a phase angle of 100° (Shoemaker and others, 1968) (table 2).

TABLE 2.—Albedo and polarimetric measurements from the Apollo 14, 11, and 12 sites and from the Surveyors 3, 5, 6, and 7 sites

	Percent albedo		Percent polarization	
	Samples	Photos	Samples	Photos
Fra Mauro				
Smooth unit soil -----	13.1	8.2-9.4	9.5	-----
Ridgy unit soil -----	-----	9.0-14.4	-----	-----
Mare Tranquillitatis soil -----	-----	9.0	20	-----
Oceanus Procellarum (Surveyor 3; Apollo 12) -----	-----	18.5	18,15	-----
Mare Tranquillitatis (Surveyor 5) -----	-----	17.9- 8.4	-----	-----
Sinus Medii (Surveyor 6) -----	-----	18.2	-----	16-19
Tycho rim (Surveyor 7) -----	-----	-----	-----	17-9

<sup>1</sup>Shoemaker and others, 1968.

Polarimetric measurements were made from four lunar soil samples: 19984,69 (Apollo 11, Mare Tranquillitatis), 12070,170 and a sample collected by Apollo 12 from the soil scoop of Surveyor 3 (Apollo 12, Oceanus Procellarum), and 14163,188 (Apollo 14, Fra Mauro). Only a few soil samples were collected by Apollo 14, and sample 14163,188 from near the LM was the only one made available for this study.

The polarization peaks of the samples are rather broad and occur at phase angles of about 100°–115° (fig. 20), slightly higher angles than the 100° peaks measured through the telescope and by the Surveyor 6 and 7

cameras. The polarization of light by the mare samples is noticeably higher than that of the Apollo 14 highlands sample. This is in general agreement with the telescopic and Surveyor measurements (table 2), and with measurements by Dollfus, Geake, and Titulaer (1971) on Apollo 12 lunar samples.

Polarization characteristics of three Fra Mauro breccias are compared with those of a mare basalt and of a soil breccia derived from mare basalt that is shown in figure 21. Although the curves for these rock samples do not have well-defined polarization peaks over phase angle ranges of 20° to 150°, and their measured maximums are widely spread with regard to their degree of polarization, the two mare samples have a considerably higher degree of polarization than the three Fra Mauro breccia samples.

Albedo measurements were taken from Apollo 14 surface photographs at traverse stations A, B, B1, B2, C', C1, G, G1, and H (pl. 2). The luminance from undisturbed surface material was measured around the shadow of the astronaut's head and shoulders, where the phase angles were 3° to 6°. The measured luminance was then extrapolated to zero phase angle luminance (albedo) by means of the lunar photometric function compiled by Willingham (1964).

The albedos of the undisturbed fine-grained surface material at the intercrater areas along the geological traverse in the smooth unit range from 8.2 to 9.4 percent (table 2). The albedo variation does not reflect a pattern but appears to be randomly distributed, except at stations G and G1, which are located on the eroded ejecta of the 150-m diameter subdued North Triplet crater (pl. 1). The materials at these stations have albedos of 9.2 to 9.4 percent, which are in the higher part of the range of albedos for the smooth unit. Stations B1 and B2, at the lower part of the ridgy unit, also have slightly higher albedos, 9.1 and 9.6 percent, respectively, which probably indicates a measureable amount of Cone crater ejecta, with higher albedo, in the materials at these stations.

The fine-grained materials in Cone crater ejecta are crushed bedrock and represent newly generated regolith. The heterogeneous fine-grained mixture of crushed light and dark banded Fra Mauro rock has albedos ranging from 10.7 to 14.4 percent. This material shows slight to undetectable darkening where disturbed by astronaut activity, in contrast to the 5 to 11 percent darkening of the regolith on the plains at stations A, B, and G.

Pohn, Wildey, and Sutton (1970) report that the albedo of the Apollo 14 landing site area ranges from 10.8 to 11.4 percent, in an integrated area of about 65 km<sup>2</sup>. The integration of small areas of bright rocks and craters probably increases the total reflectance in their

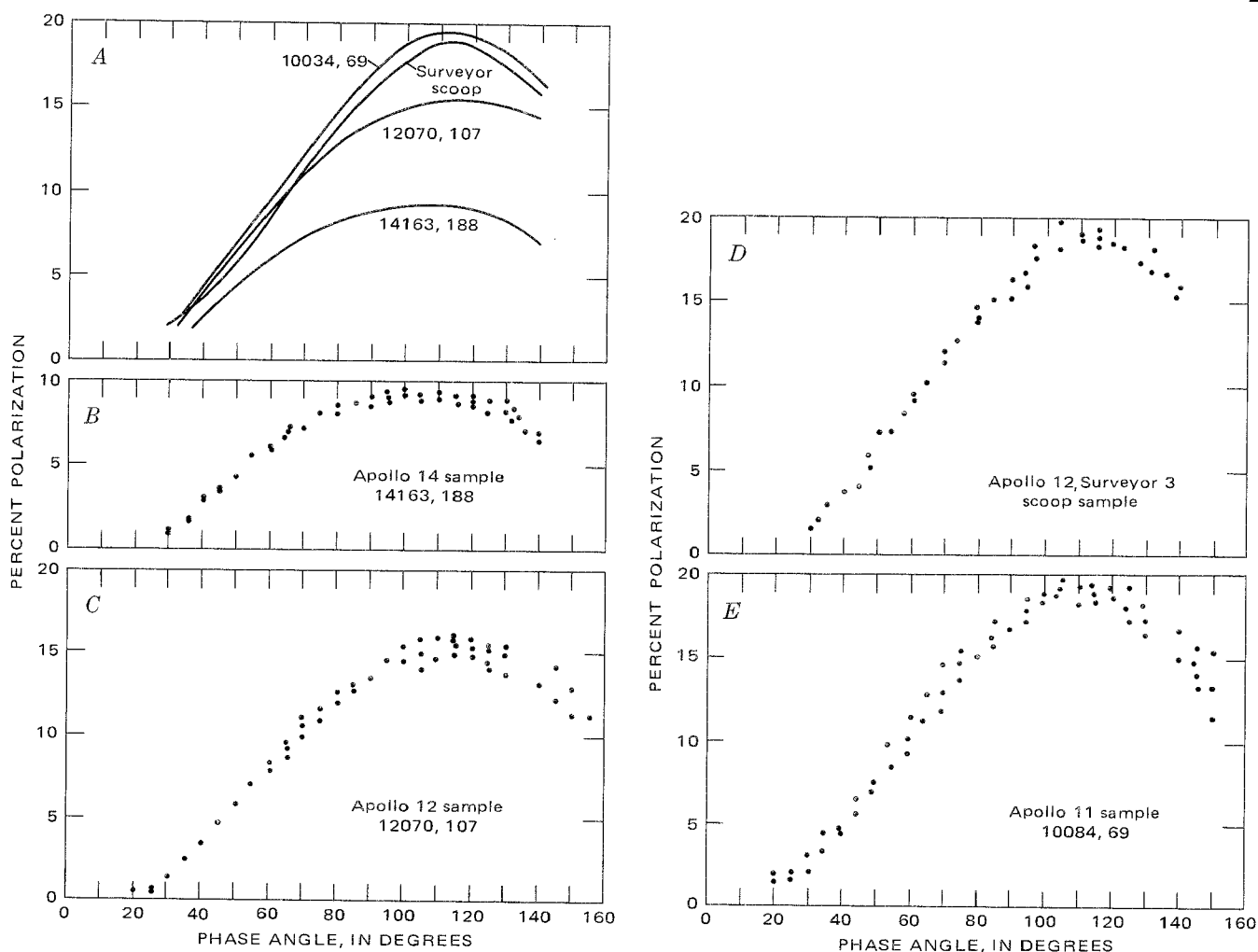


FIGURE 20.—Polarization scatter graphs of highland soil (Apollo 14) and mare soil (Apollos 11, 12, and Surveyor). A, Fit-by-eye curves comparing the scatter graph data. B, Apollo sample 14163,188. C, Apollo 12 sample 12070,107. D, Apollo 12, Surveyor 3 scoop sample. E, Apollo 11 sample 10084, 69.

measurements, compared with our spot measurements, in which bright rocks and craters were not included. The boulders of Fra Mauro material exposed on the rim of Cone crater have irregular concentrations of lighter and darker materials, which suggests that erosion of Fra Mauro rocks would initially produce a mottled regolith. The lunar regolith becomes darker with time than its parent material, probably because of increasing vitrification of regolith materials by high-energy impact (Adams and McCord, 1971). It also becomes more homogenized by mixing from repetitive impacts. The albedo of the Cone crater ejecta is representative of the broken bedrock material, and the uniformly darker material of the smooth unit represents cumulative darkening and homogenization since the Fra Mauro Formation was emplaced.

The ages derived by geochemical techniques for the Cone crater event, the North Triplet event, and the length of exposure of regolith near the LM correlate

with the albedos of the associated materials. Cone crater ejecta, which has an albedo range of 10.7 to 14.4 percent, has probably darkened little if any since its formation. North Triplet crater had an original depth of about 30 m (judging from its 150 m diameter), compared to a regolith depth of about 8.5 m, so the cratering event must have ejected fresh Fra Mauro rocks, now on the crater rim. The albedo range of 9.2 to 9.4 percent at stations G and G1, compared with the albedo of Cone crater ejecta, indicates an average of about a 3 or 4 percent darkening of the uppermost layer since the North Triplet event.

The albedo of the regolith near the LM is 8.4 percent. The exposure age for surface materials from near the LM implies that that area has not been significantly churned by cratering during the past 600 m.y. (Turner and others, 1971), and the regolith in the LM area therefore is probably not homogenized to a uniform albedo with depth. The rather uniform 8.4 percent al-

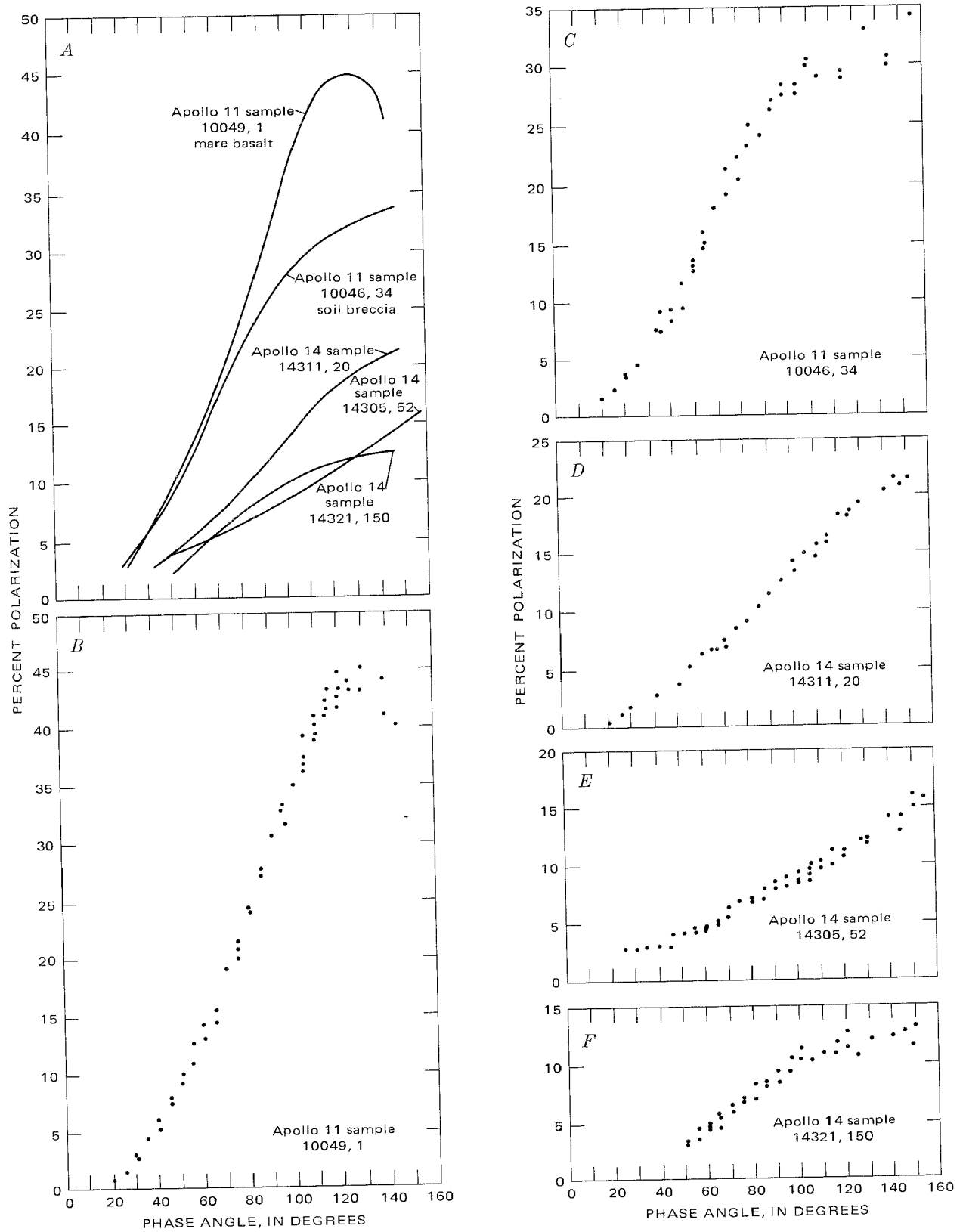


FIGURE 21.—Polarization scatter graphs of highland rocks (Apollo 14) and mare rocks (Apollo 11). A, Fit-by-eye curves comparing the scatter graph data. B, Apollo 11 sample 10049,1. C, Apollo 11 sample 10046,34. D, Apollo 14 sample 14311,20. E, Apollo 14 sample 14305,52. F, Apollo 14 sample 14321,150.

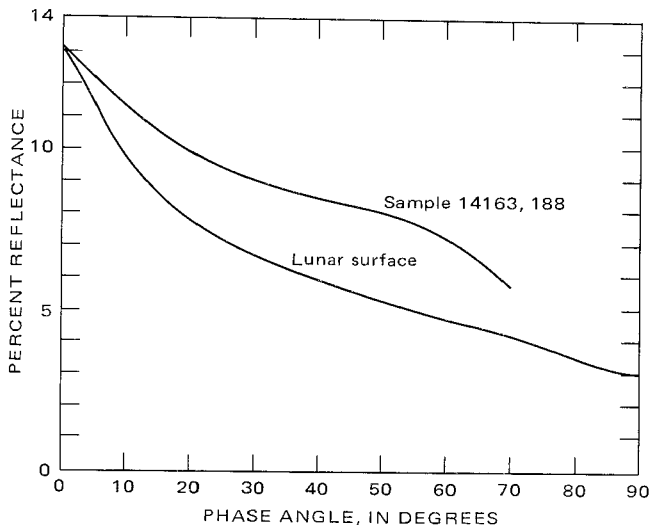


FIGURE 22.—Average reflectance of lunar surface compared with Apollo 14 soil sample 14163,188.

bedo on intercrater surface areas suggests that the additional 1 percent darkening is due to the 600-m.y. exposure age, as compared to the 100- to 260-m.y. age of North Triplet crater rim (Berdot and others, 1972). An approximation for the time required for surface layer darkening is provided by the sequential exposure ages of Apollo 14 samples. The rate of darkening appears to be initially rapid: 3 percent in about 200 m.y. with a slower rate of 1 percent in an additional 400 m.y. The heterogeneity in the albedos of Cone crater ejecta, and the relatively short exposure time of approximately 25 m.y., probably account for the inability to measure the degree of darkening of Cone crater ejecta.

The albedo of a small part of the Apollo 14 regolith bulk sample was measured in the laboratory and found to be 13.1 percent. When the sample holder was tapped, causing additional settling of the material, the albedo increased to 13.6 percent. Apparently the lunar material did not form its natural lunar microtexture in our atmosphere, and the albedo of the sample is greater than that of similar in-situ material. The regolith bulk sample was shoveled from the bottom of a 0.5-m crater reported by the astronaut crew to have a different colored layer, and it is possible that the albedo of sample 14163,188 is intrinsically higher than that of the surface, 8.4 percent. A comparison of the typical lunar photometric function with the measured function of the sample is shown in figure 22, where the lunar reflectance has a greater backscatter reflectance near zero phase angle.

The maximum albedo of 36 percent for the light parts of boulders at the Apollo 14 site is higher than any albedo that was measured on the lunar surface through the time of Apollo 14. (Muehlberger and

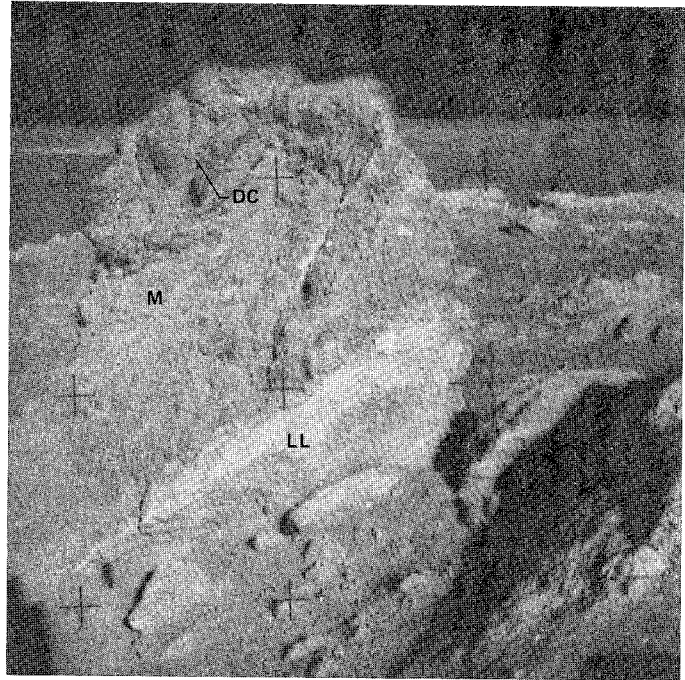


FIGURE 23.—Layered rock at station C1 showing albedo differences between dark clast (DC), matrix (M), and light layer (LL). Layered rock is about 2 m high. (NASA photograph AS14-68-9449.)

others, 1972, report albedos as high as 55 percent for South Ray crater ejecta, Apollo 16.) Layered rock in the White rocks group at station C' (fig. 23) contains dark clasts with an average albedo of 16 percent, gray matrix material with an average albedo of 20 percent, and a light-gray layer with an average albedo of 36 percent. Some light clasts such as those in Turtle rock (fig. 24) have albedos of 33 percent, about the same as that of the light layer in Layered rock. These comparable albedos imply that the light layers of the White rocks and the light clasts in some of the boulders have similar compositions.

#### GEOLOGIC STRUCTURES

There is no direct evidence for tectonic features in the landing site. Old pre-Imbrian structures, unless reactivated after the Imbrium event, would be masked by the ejecta from the Imbrium and older basins. Fractures caused by craters certainly exist in the local bedrock, but they are visible only in boulders ejected from Cone crater. However, lineaments sparsely distributed over the landing site area suggest the existence of fractures in the local bedrock.

Lineaments on the lunar surface may be grouped on the basis of size into three categories: (1) lunar grid lineaments ranging from tens to hundreds of kilometres in length, which are related to straight rilles and scarps, linear mountain fronts, and sides of large polygonal craters (Strom, 1964; Elston and others,

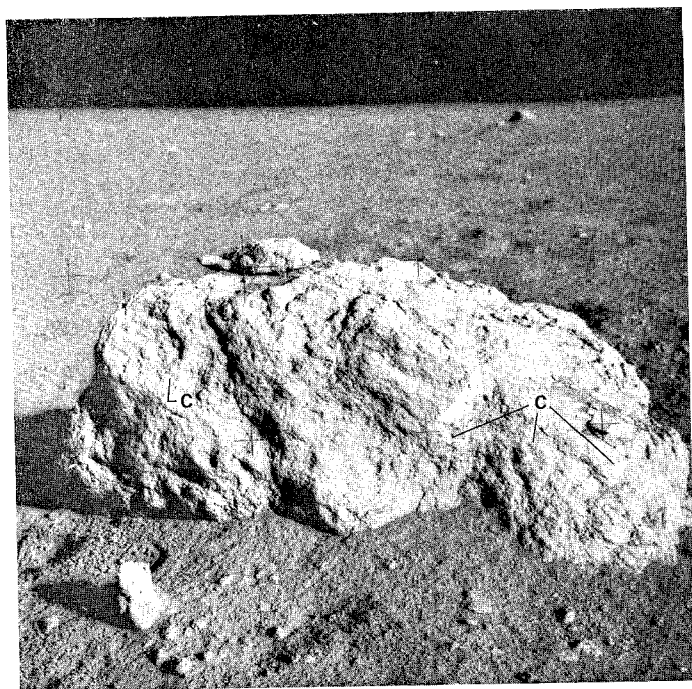


FIGURE 24.—Light clasts (C) in Turtle rock. (NASA photograph AS14-68-9476.)

1971); (2) regional-scale lineaments, ranging from tens to a few thousands of metres in length, which are elongate and commonly indistinct troughs and ridges expressed in the regolith (Carr, 1966; Schaber and Swann, 1971); and (3) small-scale lineaments ranging from a few centimetres to a few metres in length, which are also expressed as troughs and ridges in the regolith (Shoemaker and others, 1969; Schaber and Swann, 1971).

Small-scale lineaments at the Apollo 14 site that are visible in the Hasselblad photographs have two primary trends (northwest and northeast) and one secondary trend (north) (fig. 25). These features are poorly developed compared to those at the Apollo 11 and Apollo 12 sites (Schaber and Swann, 1971). The only well-defined linear features recognized on the Apollo 14 Hasselblad photographs are several features up to 100 m long that trend generally north in the vicinity of the LM (fig. 26). These unusually long lineaments, like the well-developed lineaments on the walls and rim crests of 200-m to 400-m subdued craters, may be surface reflections through the regolith of jointing in the bedrock (Schaber and Swann, 1971).

Regional-scale lineaments both at the Apollo 12 and 14 sites have northwest, northeast, north-northwest, and north-northeast trends. Apollo 12 features are about half again as abundant as those of the Apollo 14 site (fig. 27). Apollo 11 regional lineaments are about five times as abundant as those of the Apollo 14 site, but only the northwest and northeast systems are

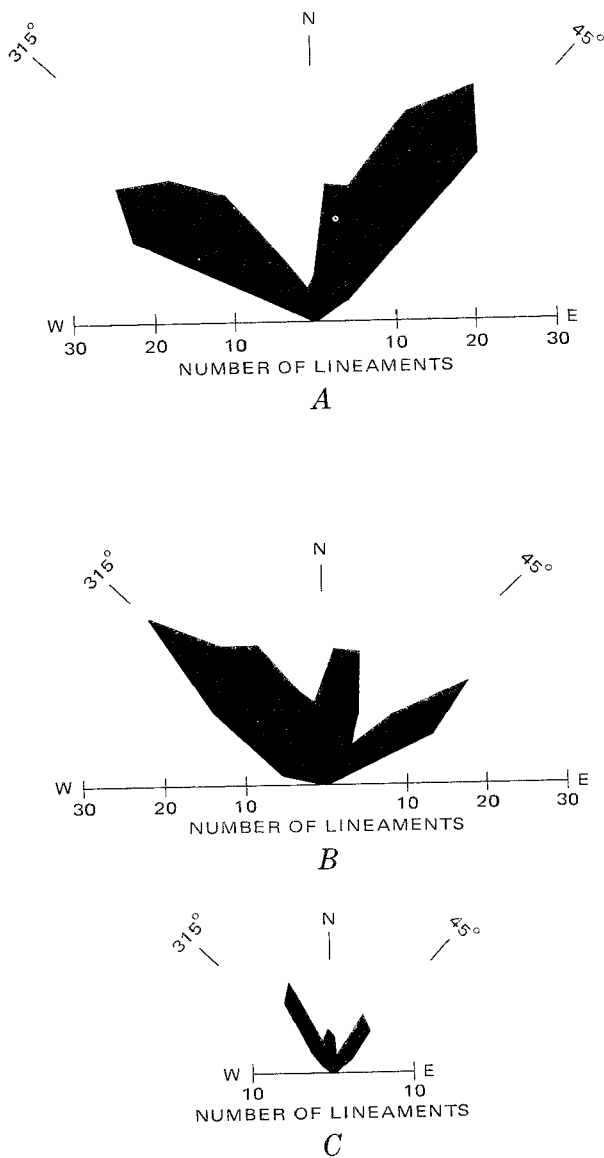


FIGURE 25.—Azimuth frequency diagrams of small-scale lineaments in the Apollo 11, 12, and 14 sites plotted from surface photographs. A, Apollo 11 (Schaber and Swann, 1971). B, Apollo 12 (Schaber and Swann, 1971). C, Apollo 14 (Swann and others, 1971).

strongly developed. A weak north-trending set is also present in the Apollo 11 regional data (fig. 27). The striking similarity of the Apollo 12 and Apollo 14 regional lineament systems may be due to the proximity of the two sites (approximately 200 km) and therefore may be a reflection of identical structural trends.

Earth-based telescopic observations of the Moon resulted in early recognition of the global system of lineaments that make up the lunar grid system. These lineaments are remarkably consistent and trend primarily northwest, northeast, and north, with less well developed north-northeast and north-northwest

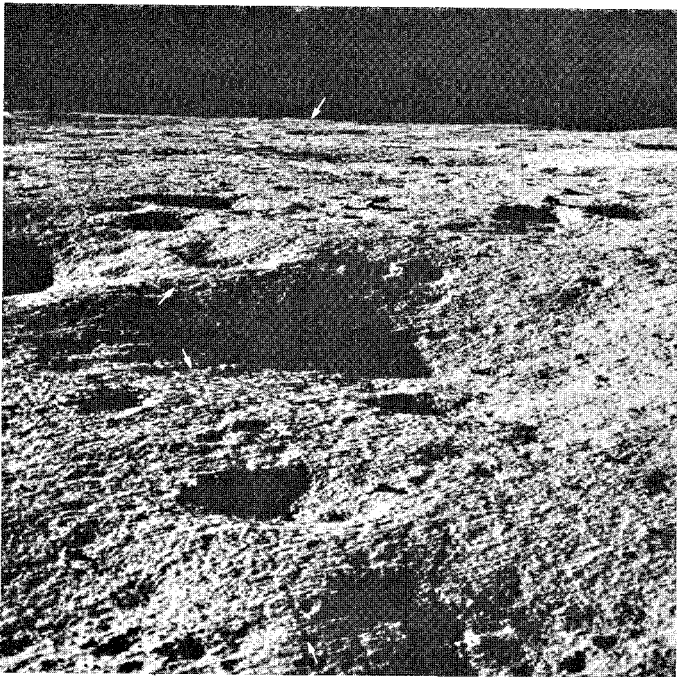


FIGURE 26.—Two long lineaments in the Apollo 14 landing site. View south. (NASA photograph AS14-66-9251.)

trends (Strom, 1964; fig. 28). Television pictures transmitted from Ranger spacecraft indicated the existence of similar lunar grid lineaments at much smaller, or regional, scale. Azimuthal trends of the regional scale lineaments largely coincide with the lunar grid (Carr, 1966). The trends of small- and regional-scale lineaments in the Apollo 11, 12, and 14 sites are also in general agreement with those of the lunar grid and, as previously suggested, may therefore be related to ancient global structural systems (Carr, 1966; Schaber and Swann, 1971).

Howard and Larsen (1972), using cupric oxide and gypsum powders and simulated lunar lighting conditions, showed that apparent lineaments can be caused by lighting effects, and Wolfe and Bailey (1972) have shown that the acute angles of the two prominent lineament trends that were observed and photographed on the Apennine front by the Apollo 15 crew are bisected by the sun azimuth. The conclusions reached by Wolfe and Bailey agree with the laboratory work of Howard and Larsen in that at least some of the strongest lineament trends (especially the northwest and northeast systems) may be effects of lighting on rough surfaces and may not represent lunar structures.

There are, however, at least three sets of lineaments in the Apollo 11, 12, and 14 traverse areas, and as many as four or five in the Apollo 12 area, and only two strong trends appear on the Apennine front and on the laboratory models. This, and the agreement in azimuthal trends with those of the lunar grid, which is

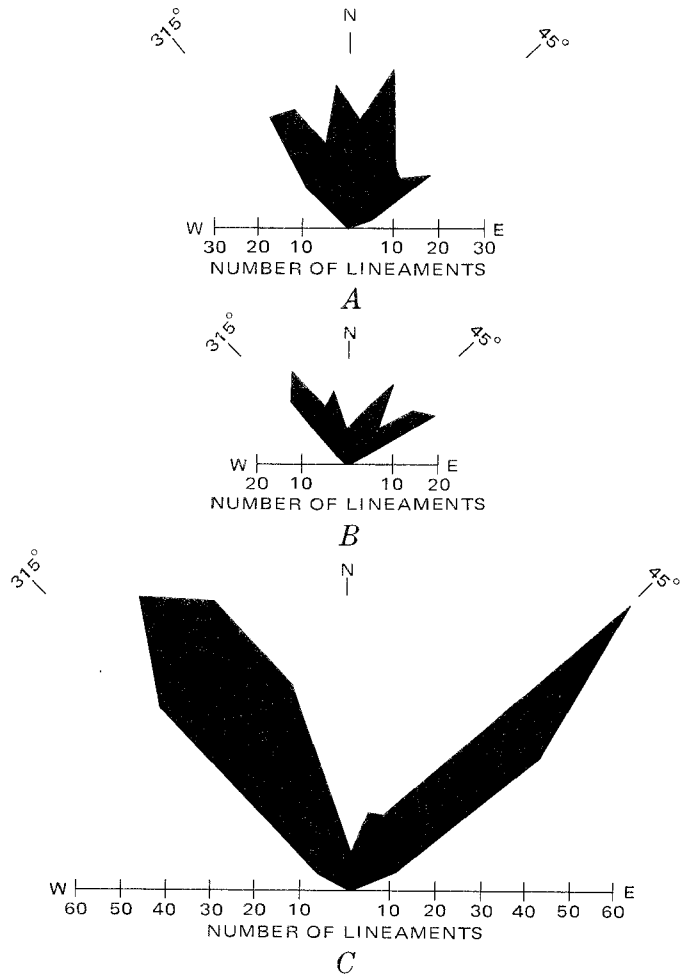


FIGURE 27.—Azimuth frequency diagrams of regional-scale lineaments in the Apollo 11, 12, and 14 landing sites. Plotted from Lunar Orbiter photographs (Schaber and Swann, 1971.)

obviously not a lighting effect, suggests that at least some of the smaller lineaments may be related to structures and are not simply effects of lighting. It is therefore suggested that when three or more sets of distinct lineaments are observed, one or more of them are actual lineaments and are not the effects of lighting.

#### FRA MAURO FORMATION

Samples of Cone crater ejecta indicate that the Fra Mauro Formation includes complex fragmental rocks derived from the brecciation of older igneous and possibly in some cases clastic rocks that predate the Imbrium event (see for example Lunar Sample Preliminary Examination Team, 1971; Swann and others, 1971; Warner, 1972; Wilshire and Jackson, 1972). Wilshire and Jackson (1972) have classified the Apollo 14 rocks into the following types:

1. Homogeneous crystalline rocks, basaltic (type B).
2. Homogeneous crystalline rocks, metaclastic (type C).

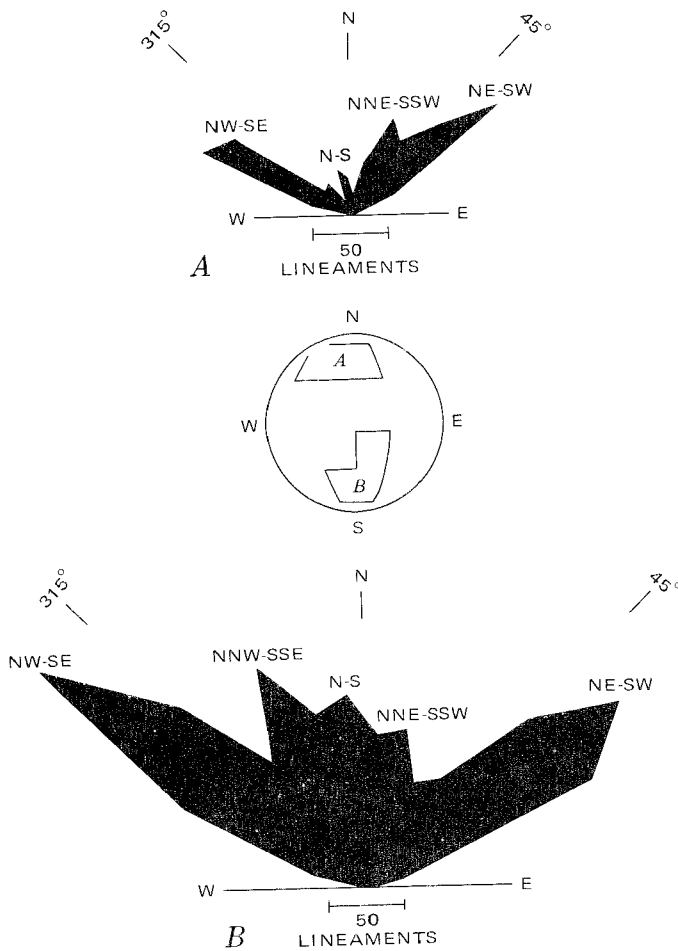


FIGURE 28.—Azimuth frequency diagram of lunar grid lineaments. *A*, Plots from northern hemisphere. *B*, Plots from southern hemisphere. The diagram represents the apparent azimuth as viewed in orthographic projection; 10,000 total plots (Strom, 1964).

3. Fragmental rocks, light clasts dominant, matrix friable (type  $F_1$ ).
4. Fragmental rocks, light clasts dominant, matrix coherent to moderately coherent (type  $F_2$ ).
5. Fragmental rocks, dark clasts dominant, matrix friable (type  $F_3$ ).
6. Fragmental rocks, dark clasts dominant, matrix coherent to moderately coherent (type  $F_4$ ).

Eggleton and Offield (1970) estimate the Fra Mauro to be about 200 m thick in the ridge areas. Kovach and Watkins (1972) interpret a 299-m/s seismic velocity layer that is estimated to range from 19 to 76 m in thickness to be the Fra Mauro Formation. We believe that variations in the degree of annealing and thus friability of Fra Mauro rocks and superposed brecciation and fracturing by post-Fra Mauro cratering events, render thickness estimates from seismic data alone unreliable. Cone crater is about 65 m deep and, therefore, if Eggleton and Offield's estimate of thick-

ness is correct, only the upper third of the Fra Mauro Formation was exposed by the Cone crater event. It is unlikely that Cone crater penetrated completely through the Fra Mauro Formation, even if Eggleton and Offield's estimate of the thickness is greatly in error. The crater missed penetrating the base of the ridge by about 30 m, and if the ridge is a depositional feature of the Imbrium ejecta blanket, then the crater could not have penetrated to the average base of the ejecta. However, a 0.75-km-diameter Eratosthenian crater immediately south of Cone crater and a 1.5-km-diameter Imbrian crater adjacent to Cone crater on the east (Eggleton and Offield, 1970) probably did penetrate to depths greater than 200 m, and therefore material would have been ejected from below the base of the Fra Mauro Formation. This material might be found any place in the landing site, and some was probably reejected by the Cone crater event. Evidence in the samples of a fossil regolith that developed on the pre-Fra Mauro surface might be the best clue as to whether samples from below the Fra Mauro were collected.

Swann and others (1971) suggested that the boulders of the White rocks group, many of which are very light colored and were observed only near the rim crest of Cone crater, may have come from the deepest level to which the crater penetrates. The samples of the White rocks are described by Wilshire and Jackson (1972) and by Chao and others (1972) as friable, and we now believe that the White rocks materials extend in the subsurface toward the northeast of Cone crater and are more friable in that direction, which accounts for the lack of boulders on the northeast rim of Cone crater. The distribution of rock types in the ejecta of Cone crater led Wilshire and Jackson (1972) to suggest that the deepest units ejected from Cone crater are composed of dark-clast fragmental rocks with friable to moderately coherent matrix (type  $F_4$  breccia; fig. 29), and that they are interlayered with light-colored, though dark-clast-dominant, fragmental rocks of the White rocks type (type  $F_3$  breccias; fig. 30). Light-clast-dominant breccias with coherent to moderately coherent matrix (type  $F_2$ ; fig. 31) are believed to have been derived from a higher part of the Fra Mauro Formation. The fragmental rocks with dominant light clasts and friable matrix (type  $F_1$ ; fig. 32) are regolith breccias derived from the uppermost target materials of Cone crater and also are formed elsewhere by impact into the regolith. Thus it is reasonable to assume that the uppermost Fra Mauro unit, the light-clast or  $F_2$ -type breccia, provided most of the regolith from which the light-clast-dominant  $F_1$ -type breccias were derived. The igneous and metaclastic rocks are probably relatively hard clasts that were eroded from the softer



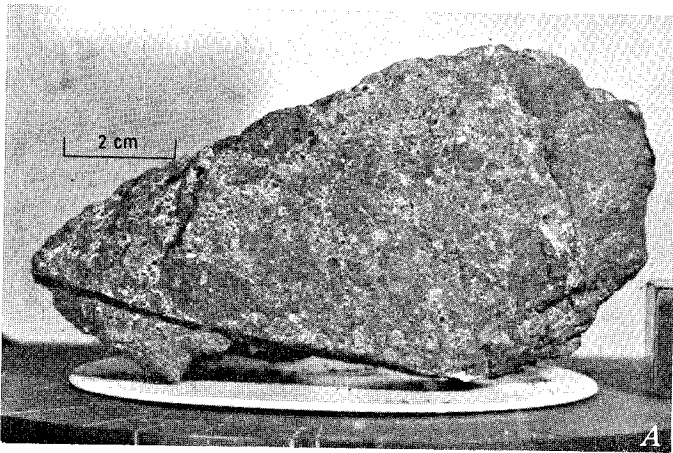
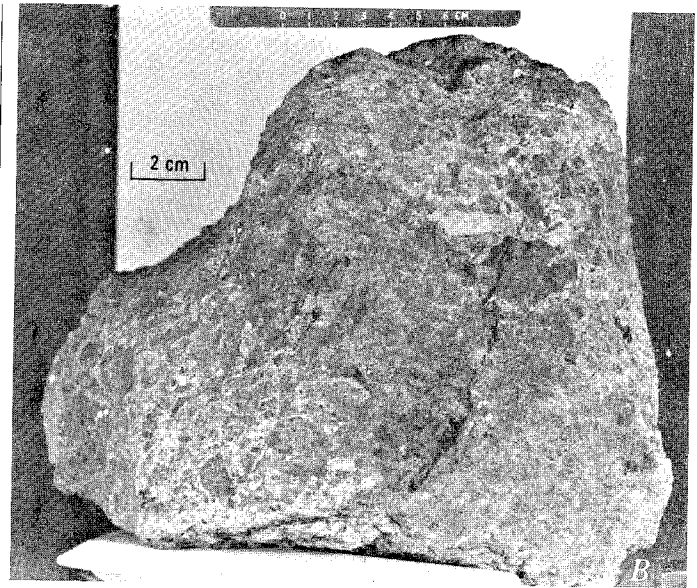


FIGURE 29.—F<sub>4</sub> breccia rock types. A, Sample 14306. Note prominent planar glass-lined fracture near bottom left. Compare with figures 68 and 69. (Part of NASA photograph S-71-22014.) B, Sample 14321, "Big Bertha." Compare with figures 76 and 77. (Part of NASA photograph S-71-22164.)



matrix breccias of the Fra Mauro Formation by micrometeorite impact.

Layering or bedding within the Fra Mauro fragmental rocks can be seen in photographs of several of the large boulders at the Apollo 14 site. In addition, many of the same kinds of structures, such as layering and fracturing, are found in the samples (fig. 29).

Samples 14053, taken from a boulder at station C2, and 14068, collected at station C' (pl. 2), may be representative of materials from the base of the Fra Mauro Formation. Sample 14053 is a coarse-grained gabbroic rock with silicon- and potassium-rich glass in its interstices. It is somewhat similar in composition and texture to some of the crystalline rocks returned by Apollo 12, and may therefore be a mare-type basalt (Kushiro and others, 1972; Lovering and others, 1972; Chao and others, 1972). Schürmann and Hafner (1972)

conclude that the rock was heated by impact events, probably at the Imbrium basin site, and was later quenched, probably in a cold regolith, at the Fra Mauro site. The large boulder does appear friable in the photographs (Schürmann and Hafner, 1972), but when Astronaut Mitchell failed to break a sample with the hammer, he exclaimed "No, man; that's hard, hard, hard." Shepard then picked a loose piece (sample 14053) off the opposite side of the rock. If Schürmann and Hafner's interpretation is correct, the boulder appears to be an unusually coarse and well-annealed regolith breccia.

Sample 14068, studied in detail by several investigators, is reported by Warner (1972) to be a high-grade metamorphic breccia with no, or only a trace of,

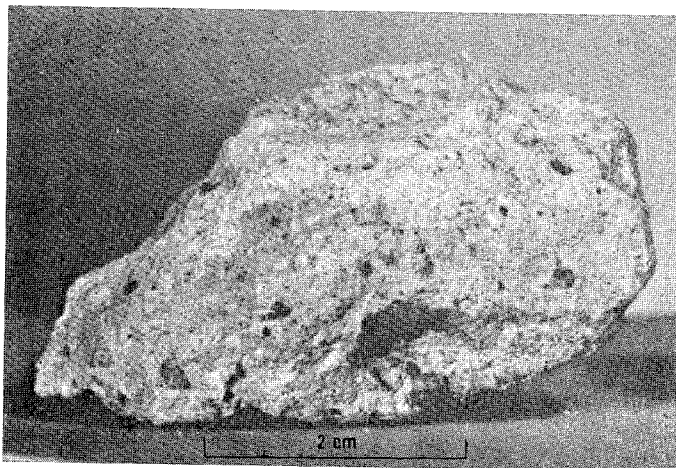


FIGURE 30.—F<sub>3</sub> breccia rock type. Sample 14082. Compare with figures 59 and 60. (Part of NASA photograph S-71-32443.)

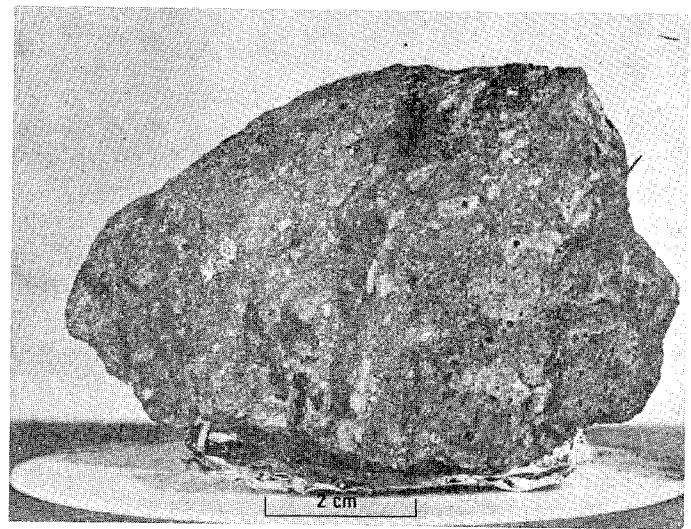


FIGURE 31.—F<sub>2</sub> breccia rock type. Sample 14318. Note zap pits (Z) on surface and dark glass coating (G) near lower center. Compare with figures 74 and 76. (Part of NASA photograph S-71-22016.)

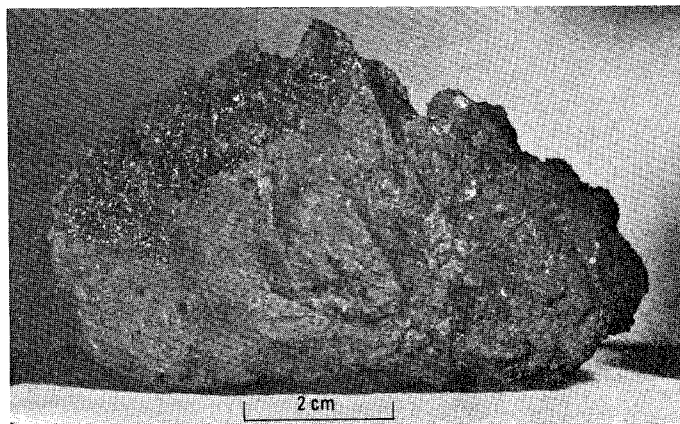


FIGURE 32.—F<sub>1</sub> breccia rock type. Sample 14047. Note glass coating on upper left. Compare with figures 51 and 52. (Part of NASA photograph S-71-21452.)

glass in the matrix and no glass clasts, that melted at a temperature greater than 1,000° C. Nelen, Noonan, and Fredriksson (1972) report that the rock has a fine-grained, quenched texture, and Helz (1972) reports a cooling regime similar to that of sample 14053. Helz's additional observation of dark microbreccia rimming parts of 14068, together with its similarities to 14053, suggests that if Schürmann and Hafner's interpretation is correct, sample 14068 may also have been quenched in a cold (presumably pre-Fra Mauro) regolith, part of which annealed to the rock to form the dark microbreccia. The chemical composition of the major elements of the microbreccia (Helz, 1972) is similar to the average composition of Apollo 14 fines (Compston and others, 1972a). This supports the hypothesis that 14068 may have been quenched in the pre-Fra Mauro regolith, but only if the pre-Fra Mauro regolith, probably formed from ejecta from other large basins, is similar in composition to the present regolith on the Fra Mauro.

If these two samples do represent material from the pre-Fra Mauro regolith, they probably were ejected from a crater large enough to penetrate to the base of the Fra Mauro Formation, and later ejected from Cone crater. An exposure age of up to 30 m.y. based on the <sup>38</sup>Ar/<sup>37</sup>Ar ratio has been reported for sample 14053 (Turner and others, 1971). This is consistent with other ages reported for the Cone crater impact and suggests that if the rock were excavated by a pre-Cone crater event, then it was reburied, presumably by ejecta from the same event. No exposure age has been reported for sample 14068 that we know of.

Sample 14072, collected at station C', was studied in detail by several investigators, and is reported by Bence and Papike (1972), Longhi, Walkder, and Hayes (1972, p. 131), and Steele and Smith (1972, p. 973) to be similar in texture and mineralogy to sample 14053 and

to several Apollo 12 basalts.

The <sup>40</sup>Ar-<sup>39</sup>Ar age given for sample 14053 (Turner and others, 1971) is 3.93 ± 0.05 b.y., which is consistent with the age of formation of the Imbrium basin (see for example Nyquist and others, 1972). Compston and others (1972a), on the basis of a rubidium-strontium age suggest that sample 14072 could have a crystallization age as great as 4.06 b.y., and York, Kenyon, and Doyle (1972), on the basis of a <sup>40</sup>Ar-<sup>39</sup>Ar age, suggest that 14072 may have crystallized 4.04 ± .05 b.y. ago. It is not clear, however, to what extent the radiogenic clocks were reset by the Imbrium event (see for example Compston and others, 1972a), and age variations of Fra Mauro materials that range from the age of the Imbrium event to some earlier period of time are to be expected. The composition and radiogenic ages of samples 14053 and 14072 are evidence of the existence of mare-type basalts in the Imbrium target materials before the basin formed.

Although there appears to be general agreement among various workers that the F<sub>1</sub> breccias of Wilshire and Jackson are regolith or soil breccias (Chao and others, 1972; Warner, 1972), there is some disagreement as to the origin of some following F<sub>2</sub> breccias. Chao, Minkin, and Best (1972), Quaide and Wrigley (1972), and Floran, Cameron, Bence, and Papike (1972) all interpret sample 14313 to be a soil breccia. Juan, Chen, Huang, Chen, and Wang Lee (1972), however, suggest that the presence of undeformed glass spherules in the sample indicates that it was not formed by shock lithification. Von Englehardt, Arndt, Stoffler, and Schneider (1972) and Quaide and Wrigley (1972) interpret sample 14318 to be a soil breccia.

This could shed some doubt as to the existence of the F<sub>2</sub> unit of Wilshire and Jackson by suggesting that what they interpret as F<sub>2</sub> breccias, as well as the F<sub>1</sub> breccia, are actually soil breccias formed in regolith that was derived from the Fra Mauro Formation. However, as Wilshire and Jackson point out, the clast population of the F<sub>2</sub> breccias is markedly different from that of the dominant F<sub>4</sub> breccias, which indicates that the F<sub>2</sub> breccias could not be derived from an F<sub>4</sub> breccia parent. The difficulty probably lies in distinguishing soil breccias derived from F<sub>2</sub> breccia from the parent F<sub>2</sub> breccia itself.

Sample 14305, an F<sub>4</sub> breccia, lies on the north edge of a small, sharp, irregular depression that appears to have been formed by impact of rock 14305, the lower southwest edge of the rock having formed the major part of the depression (fig. 33). The vertical southwest edge of the rock appears to have formed the northeast-trending, grooved part of the depression as the rock slid to the northeast. A small fillet approximately 1 cm deep lies against the southeast edge of the rock, as